Validation of a real-time model-based approach for ITER first wall heat flux control on the TCV tokamak

H. Anand[1], R. A. Pitts[1], P. C. de Vries[1], J. A. Snipes[1], F. Nespoli[3], C. Galperti[2], R. Maurizio[2] S. Coda[2], B. Labit[2], I. Nunes[1], M. Brank[4], L. Kos[4], L. Zabeo[1], Y. Gribov[1], G. Simic[4]

[1] *ITER Organization, St.-Paul-lez-Durance Cedex, France*

[2] *Swiss Plasma Center (SPC), Lausanne, Switzerland*

[3] *Aix Marseille University, CNRS, Marseille, France*

[4] *University of Ljubljana, Ljubljana, Slovenia*

Introduction

The use of water cooled plasma facing components (PFCs) during burning plasma operation in ITER, imposes limits on the heat flux deposition. Thus, a robust and reliable real-time (RT) monitoring and control of PFC heat fluxes is mandatory for the ITER tokamak. At ITER, the monitoring and protection of PFCs will be performed by the wide angle viewing system (WAVS) comprising visible (VIS) and infrared (IR) cameras. A sophisticated off-line field line tracer package, SMITER (uses the SMARDDA [1] kernel) has also been successfully developed to allow power deposition mapping on the full 3D CAD geometry of ITER. The demanding computational load restricts its application in RT, so a control oriented heat flux monitoring system accounting for the effect of 3D PFCs, based on Matlab/Simulink software [3] was developed for the ITER plasma control system (PCS) [2].

The validation and verification of the proposed algorithm for limiter plasma configurations on TCV tokamak is reported [4].

Experimental analysis

A dedicated set of limiter Ohmic plasma discharges has been performed to verify the performance of the control oriented model for estimating the power flux on the inner wall of the TCV tokamak. The main diagnostic used in the experimental testing is the horizontal (HIR) infrared camera [6]. The view of the HIR, an example of the magnetic equilibrium (# 51399) and the corresponding deposited heat flux, q_{dep} on a inner wall tile are shown in Fig. 1. The deposited heat flux is modelled as the sum of heat flux components perpendicular, $q_{dep,\perp} = q_{\perp}(r_u)cos(\alpha)$ and parallel, $q_{dep,||} = q_{||}(r_u)sin(\alpha)$ to the magnetic field line and a background component. The parallel, $q_{||}(r_u)$ and perpendicular, $q_{\perp}(r_u)$ heat flux radial profile at the outer midplane is

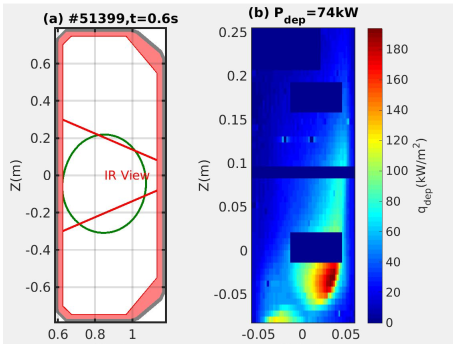

Figure 1: *(a) Example of a plasma magnetic equilibrium used in the analysis. The field of view of the HIR system is shown by the red solid lines. (b) Deposited heat flux obtained from IR images.*

computed by utilising simplified methods for the determination of the wetted area and field line angles [7]. The result of the analysis is shown in Fig. 2. The sum of the deposited power, amounts to ≈ 65 % of the exhausted power across the plasma boundary, P_{SOL} [6].

The power corresponding to perpendicular component of the heat flux (Fig. 2(b)) contributes ≈35 % of the total deposited power on the tile surface [8]. Since, SMITER and the model-based approach assumes only heat flow parallel to magnetic field lines, the resulting heat flux distribution from the codes would be compared only to the parallel component of deposited heat flux derived from IR images (Fig. 2(a)). The specifications for the parallel heat flux profile in the SOL are obtained experimentally from the IR images following the instructions mentioned in [8]. The measured profile and parameters obtained by fitting the data with a double exponential are shown in Fig. 3 for # 51399 [9].

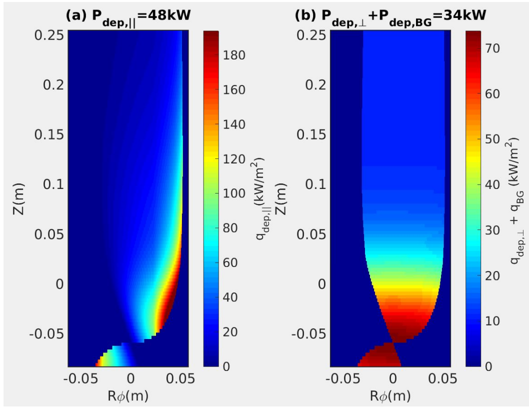

Figure 2: *(a) Modelled components of the deposited heat flux parallel to the magnetic field and (b) sum of the background heat flux and component perpendicular to the magnetic field.*

Accounting for 3D PFCs

A realistic value of the heat flux can only be obtained by accounting for the 3D geometry of the PFCs. This is achieved by studying the off-line heat flux distribution on the TCV inner wall tiles using SMITER. The determination of the power flux density is obtained by 3D field line tracing for a given magnetic equilibrium to compute the plasma wetted area, while accounting for shadowing by neighbouring components (including self-shadowing).

For the given magnetic equilibrium (Fig. 1(a)), component of the deposited power parallel to the magnetic field line, $P_{dep,||}$ and specification for the heat flux profile (Fig. 3) obtained from the deposited heat flux, SMITER is used to simulate the surface heat loads. Fig. 4 shows the heat load distribution obtained with SMITER and its the comparison with the modelled deposited heat flux at various toroidal and poloidal cuts. The toroidal and poloidal heat flux profiles are in good agreement (Fig. 4(b-e)). However, the discrepancy in the profiles can be compensated by imposing the wetted area and field line angles computed by SMITER while determining the parallel component of the deposited heat flux on the TCV central column.

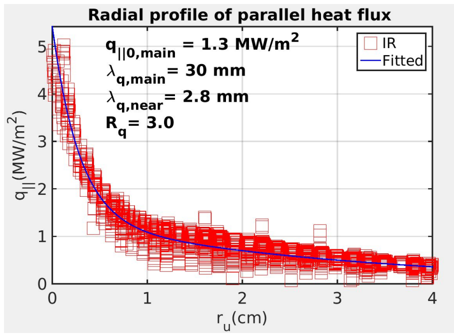

Figure 3: *Parallel heat flux profile (red square), fitted with a double exponential function (blue line).*

Model-based power flux estimation

The Matlab/Simulink architecture of the wall heat flux estimator for ITER has been adapted to estimate the power flux density on the TCV central column tiles. The model is implemented on a dedicated core of a multi-core computational node of the TCV digital control system [5] and cycles at a sample time of 0.6 ms. The fundamentals of the control oriented model are described in [3].

For each plasma equilibrium, the magnitude of the peak heat flux from SMITER and model-based approach is determined and the associated weighting factor, W_F, defined as the ratio of the peak power flux density obtained from SMITER and the model-based approach is calculated. The comparison between the heat flux distribution obtained from SMITER and model-based approach for different limiter plasma configurations varying in plasma elongation is shown in Fig. 5. As expected, the power flux distribution between SMITER and model-based approach are in good agreement at the apex of the tile (Fig. 5(b-d)).

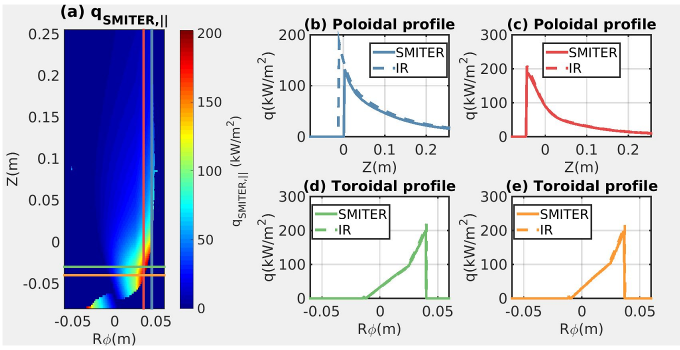

Figure 4: *(a) Heat flux distribution derived from SMITER and location of toroidal and poloidal cuts used for comparing the heat flux profile. Comparison between heat flux distribution derived from the IR measurements and SMITER at various poloidal ((b) and (c)) and toroidal cuts ((d) and (e)).*

However, It is evident that the model assuming a cylindrically symmetric first wall underestimates the magnitude of the peak heat flux (Fig. 5(b-d)) and, of course, has no knowledge of its toroidal localization (it has knowledge only in the poloidal plane). The dependency of the weighting factor with plasma elongation, for different plasma equilibria is shown in Fig. 5(e). The average value of the weight factors is implemented in the algorithm to include the 3D geometry of the inner wall tiles.

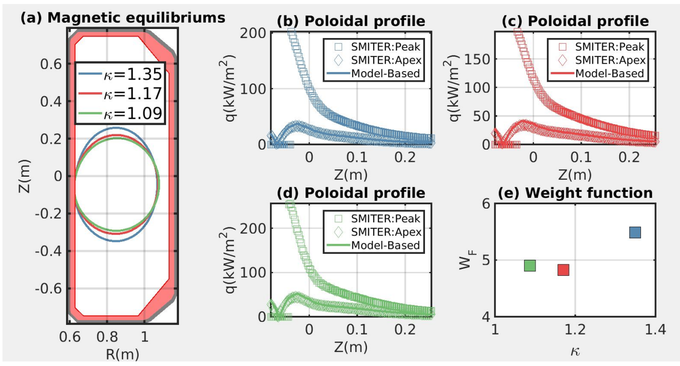

Figure 5: *(a) Different plasma magnetic equilibria used for estimating the heat flux distribution from SMITER and the model-based approach. (b-d) Poloidal profiles of the inner wall heat flux density for the equilibria in (a). (e) Evolution of the weight function with plasma elongation.*

The application of the algorithm for estimating the heat flux distribution on TCV for limiter (#51392) plasma discharge is shown in Fig. 6. Good agreement between the peak heat flux and its location in the poloidal plane derived from the IR images and model-based approach for a limiter plasma configuration was observed.

Summary

A successful experimental implementation of the wall heat flux estimator algorithm has been demonstrated at TCV tokamak. Good agreement with the IR camera is achieved with respect to estimation of the peak heat flux and its location in the poloidal plane for limiter plasma discharges. The heat load distribution on the TCV central column tiles derived using the SMITER GUI is successfully benchmarked against the deposited heat flux measured by the IR camera. The experimental validation of the model based approach accounting for 3D effects of the plasma facing components on TCV demonstrates the RT operational feasibility of the wall heat flux algorithm developed for ITER.

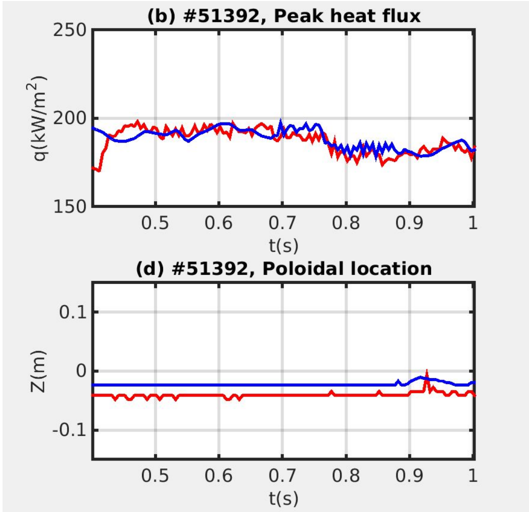

Figure 6: *Evolution of the peak heat flux and its location in the poloidal plane using model-based approach and IR analysis.*

Disclaimer

The views and opinions expressed herein do not necessarily reflect those of the ITER Organization.

This work was supported in part by the Swiss National Science Foundation

This work has been carried out within the framework of the EUROfusion Consortium and has received funding from the Euratom research and training programme 2014-2018 under grant agreement No 633053. The views and opinions expressed herein do not necessarily reflect those of the European Commission.

References

[1] Arter W et al., IEEE Transactions on Plasma Science, **42**, 1932 (2014)
[2] Walker M et al., Fusion Engineering and Design, **89**, 518 (2015)
[3] Anand H et al., Fusion Engineering and Design (submitted) ,(2018)
[4] Coda S et al., Nuclear Fusion , **57**, 12, (2017)
[5] Anand H et al., Nuclear Fusion , **57**, 56005 (2017)
[6] Maurizio R et al., Nuclear Fusion , **58**, 16052 (2018)
[7] Nespoli F et al., Journal of Nuclear Materials , **463**, 393 (2015)
[8] Nespoli F et al., Nuclear Fusion , **57**, 126029 (2017)
[9] Kocan M et al., Nuclear Fusion , **55**, 33019 (2015)
[10] Eich T et al., PRL , **107**, 215001 (2011)